HHS Public Access

Author manuscript

Neurobiol Dis. Author manuscript; available in PMC 2018 June 01.

Published in final edited form as:

Neurobiol Dis. 2017 December ; 108: 73–82. doi:10.1016/j.nbd.2017.08.006.

Intravenous immune-modifying nanoparticles as a therapy for spinal cord injury in mice

Su Ji Jeong[a,1], **John G. Cooper**[a,1], **Igal Ifergan**[b,1], **Tammy L. McGuire**[a], **Dan Xu**[b], **Zoe Hunter**[b], **Sripadh Sharma**[a], **Derrick McCarthy**[b], **Stephen D. Miller**[b,*], and **John A. Kessler**[a,*]

[a]Department of Neurology, Northwestern University Feinberg School of Medicine, Chicago, IL 60611, USA

[b]Department of Microbiology-Immunology and the Interdepartmental Immunobiology Center, Northwestern University Medical School, Chicago, IL 60611, USA

Abstract

Intravenously infused synthetic 500 nm nanoparticles composed of poly(lactide-*co*-glycolide) are taken up by blood-borne inflammatory monocytes via a macrophage scavenger receptor (macrophage receptor with collagenous structure), and the monocytes no longer traffic to sites of inflammation. Intravenous administration of the nanoparticles after experimental spinal cord injury in mice safely and selectively limited infiltration of hematogenous monocytes into the injury site. The nanoparticles did not bind to resident microglia, and did not change the number of microglia in the injured spinal cord. Nanoparticle administration reduced M1 macrophage polarization and microglia activation, reduced levels of inflammatory cytokines, and markedly reduced fibrotic scar formation without altering glial scarring. These findings thus implicate early-infiltrating hematogenous monocytes as highly selective contributors to fibrosis that do not play an indispensable role in gliosis after SCI. Further, the nanoparticle treatment reduced accumulation of chondroitin sulfate proteoglycans, increased axon density inside and caudal to the lesion site, and significantly improved functional recovery after both moderate and severe injuries to the spinal cord. These data provide further evidence that hematogenous monocytes contribute to inflammatory damage and fibrotic scar formation after spinal cord injury in mice. Further, since the nanoparticles are simple to administer intravenously, immunologically inert, stable at room temperature, composed of an FDA-approved material, and have no known toxicity, these findings suggest that the nanoparticles potentially offer a practical treatment for human spinal cord injury.

Keywords

Spinal cord injury; Fibrosis; Gliosis; Monocyte; Macrophage; Nanotechnology

[*]Corresponding authors at: Northwestern University, 303 East Chicago Avenue, Chicago, IL 60611-3008, USA. s-d-miller@northwestern.edu (S.D. Miller), jakessler@northwestern.edu (J.A. Kessler).

[1]These authors contributed equally to this work.

1. Introduction

Traumatic injury to the spinal cord (SCI) disrupts the blood-brain barrier and leads to a cascade of secondary responses including a rapid influx of monocytes into the injured area. Monocyte infiltration occurs in a biphasic pattern (Berton and Lowell, 1999; Boros et al., 2010; Shantsila et al., 2011) that begins within hours after SCI. The number of macrophages peaks at 7 days with a second peak at 14–28 days post injury. Infiltrating monocytes, as well as tissue resident microglia, differentiate into macrophages (Fleming et al., 2006; Beck et al., 2010; David and Kroner, 2011). Monocytes and macrophages/microglia in the injured spinal cord have both detrimental and beneficial actions, and the exact roles of these populations after SCI are yet to be fully elucidated (Meda et al., 1995; Popovich et al., 1999; Popovich et al., 2002; Majed et al., 2006; Letellier et al., 2010). Recent studies suggest that the early influx of hematogenously-derived macrophages (hMΦ), but not macrophages derived from resident microglia (mMΦ), is primarily responsible for secondary axonal dieback after SCI (Beck et al., 2010; Durafourt et al., 2012; Evans et al., 2014; Gensel and Zhang, 2015). Thus, selectively blocking hMΦ infiltration during the early phase of SCI without altering microglia could help limit secondary tissue damage while preserving the beneficial effects of mMΦ.

The tools used in prior studies of monocyte/macrophage depletion do not exclusively target only hMΦ. Clodronate liposomes, when injected intravenously, deplete circulating monocytes and improve motor functions after SCI in rodents (Popovich et al., 1999; Horn et al., 2008; Grosso et al., 2014). However, clodronate liposomes also target and destroy CNS resident microglia (Kumamaru et al., 2012; Plemel et al., 2014), which may reduce the beneficial effects exerted by microglia in the damaged spinal cord. CCR2 antagonists (Kang et al., 2011), and CCR2 small interfering RNA (Leuschner et al., 2011) target hematogenous monocytes and may spare microglia which do not express CCR2 (Jung et al., 2009; Mizutani et al., 2012). However, this approach also targets T cells and immature B cells that express CCR2 (Mack et al., 2001; Flaishon et al., 2004). There are similar issues with other techniques that have been used to reduce macrophage infiltration after SCI (Mabon et al., 2000; Fiore et al., 2004; Stirling et al., 2004; Lopez-Vales et al., 2005).

Here, we sought to selectively deplete hΦM after SCI by using intravenously injected biodegradable carboxylated poly(lactide-*co*-glycolide) (PLGA) immune-modifying nanoparticles (IMPs). IMPs are highly negatively charged, synthetic, 500 nm-diameter particles that bind to the macrophage receptor with collagenous structure (MARCO) on monocytes. IMPs are immunologically inert and simple to manufacture (Getts et al., 2012). We chose to use 500 nm diameter particles because a previous study reported that 500 nm diameter microparticles have a higher binding affinity for MARCO than microparticles with 20 nm, 200 nm, or 1000 nm diameters (Sanae Kanno and Hirano, 2007). Monocytes bound to IMPs no longer travel to sites of inflammation, but instead are sequestered in the spleen where they undergo cas-pase-3 mediated apoptosis (Getts et al., 2014). IMPs reduce tissue damage and improve outcomes in animal models of several inflammatory diseases including encephalomyelitis, lethal flavivirus encephalitis, myocardial infarction, dextran sodium sulfate–induced colitis, and thioglycollate-induced peritonitis (Getts et al., 2012; Getts et al., 2014).

SCI leads to scarring at the lesion site that includes both fibrotic and gliotic responses (Goritz et al., 2011; Soderblom et al., 2013; Zhu et al., 2015a; Zhu et al., 2015b). The lesional scar inhibits axonal regeneration through a number of mechanisms including accumulation of molecules that are inhibitory to axonal outgrowth, such as chondroitin sulfate proteoglycans (CSPGs), and acting as a physical impediment to axon elongation. The relative roles of gliosis and fibrosis in inhibiting axon outgrowth are unclear. Traditionally astrogliosis has been viewed as an impediment to axon outgrowth, but some evidence suggests that certain populations of astrocytes could enhance regeneration after SCI (Bush et al., 1999; Faulkner et al., 2004; Anderson et al., 2016). The fibrotic response appears to arise from perivascular fibroblasts, which secrete the majority of fibronectin in spinal lesions (Goritz et al., 2011; Soderblom et al., 2013; Zhu et al., 2015a; Zhu et al., 2015b). Secreted fibronectin dimers are then assembled into an insoluble fibronectin matrix via an integrin dependent mechanism. The assembled matrix is characterized by abundantly crosslinked fibronectin that fails to be successfully remodeled and has been shown to remain even at chronic time points after SCI (Zhu et al., 2015b). In toto these observations suggest that both gliosis and fibrosis at the lesion site influence regenerative responses after SCI.

In this paper, we report that IMPs administered intravenously (iv) after SCI significantly reduced numbers of intralesional inflammatory macrophages and other hematogenous inflammatory cells and decreased the proportion of M1-polarized inflammatory macrophages. IMPs did not bind to resident microglia, and IMPs treatment after SCI did not change the number of microglia in the injured spinal cord. hMΦ depletion via IMPs treatment diminished fibrotic scarring and collagen accumulation in the injured sites, suggesting a relationship between hematogenous monocytes and chronic fibrotic scarring. IMPs treatment did not alter glial scarring but did reduce accumulation of chondroitin sulfate proteoglycans in the scar. Moreover, IMPs treatment significantly improved recovery of motor function in mouse models of both moderate and severe SCI. IMPs are simple to administer intravenously, are stable at room temperature for up to several months, are composed of an FDA-approved material and have no known animal toxicity. The outstanding translatability of IMPs, combined with our animal data, suggests that IMPs potentially offer a practical treatment for human SCI.

2. Materials and methods

2.1. Experimental design

The present work adheres to the ARRIVE guidelines and the Minimal Information about a Spinal Cord Injury Experiment reporting standards (Kilkenny et al., 2010; Lemmon et al., 2014). The objectives of this study were to define the role of hMΦ in glial and fibrotic scarring and to determine whether IMPs treatment improves anatomic and functional recovery after SCI in mice. All experiments in this paper were conducted with the researchers blinded to the identity of the treatment groups. One researcher, who did not participate in the behavioral scoring or tissue analyses, randomized and administered the treatment injections and maintained the blinding key. Samples were unblinded only after all measurements were completed. The number of animals in each group necessary for each measurement was determined by a power analysis done with G*Power 3.1.9.2 using the

standard deviations and effect sizes from our preliminary studies, an alpha of 0.05, and a power (1-β) of 0.80. Flow cytometry data, except for M1 and M2 macrophage analysis, was replicated with three independent experiments. M1 and M2 macrophage flow cytometry was done twice.

2.2. Mouse spinal cord injury and care

All animal procedures were performed in accordance with the Public Health Service Policy on Humane Care and Use of Laboratory Animals and were approved by the Northwestern University Institutional Animal Care and Uses Committee. Eight-week old female C57BL/6 mice (Charles River) were anesthetized using 2.5% isoflurane gas in oxygen. A laminectomy was performed to expose the spinal cord at the T11 level. A severe injury was performed using the Infinite Horizons Spinal Cord Impactor system (IH-0400 Precision Systems and Instrumentation) with 100 kdyn of impact force and a dwell time of 60 s. A moderate injury was induced with 60 kdyn of impact force and zero dwell time. After the injuries, the skin was sutured using 9 mm wound clips (BD Biosciences) and the animals were allowed to recover on a heating pad to maintain body temperature. Buprenorphine anesthetic (0.05 mg/kg, subcutaneously in 1 ml sterile saline) was administered daily for two days after injury. Baytril antibiotic (2.5 mg/kg, subcutaneously in 1 ml sterile saline) was administered daily for three days after injury to reduce the risk of infection. Bladders were manually expressed daily.

2.3. IMPs injection

Five-hundred-nanometer carboxylated PLG microparticles were obtained from Phosphorex, Inc. (Fall River, MA) and diluted in sterile phosphate buffered saline (PBS, pH = 7.4) to a final concentration of 4.7 mg/ml. 200 μl of the dilute IMPs was injected via tail vein 2–3 h after SCI. Additional injections were performed at 24 and 48 h post injury. Control animals received equivalent volume injections of sterile PBS at the same time points.

2.4. Open field testing

Fifty mice (25 per group) were injured for each experiment. Behavioral scoring was performed 24 h after injury using Basso Mouse Scale (BMS) open field scoring by two researchers blinded to the identity of the treatment groups. Any animal with a combined BMS score (left hindlimb + right hindlimb) greater than one at 24 h post injury was excluded from further analysis. Thereafter, BMS scores were assessed weekly by two blinded investigators. Graphs presenting detailed behavioral recovery data and score distributions were prepared in the style of (Estrada et al., 2014).

2.5. Flow cytometry

Mice were anesthetized with 50 mg/kg Nembutal followed by cardiac perfusion with 30 ml of PBS. Injured sections of spinal cords were pooled (four to six mice/experiment), minced with a razor, pushed through a 100 μm filter and digested at 37 °C for 60 min in a PBS solution containing 40 U/ml of Liberase R1 (Roche) and 50 mg/ml DNase I. The same technique was applied to the non-injured sections (lumbar region) of spinal cords. The resulting cellular suspension was resuspended in 30% Percoll, overlayed onto 70% Percoll

and centrifuged at 1500 rpm for 25 min at 25 °C. Cells at the interface were collected, washed, resuspended in FACS buffer (PBS with 2% FCS) and counted. The number of cells in each subpopulation was determined by multiplying the percentage of lineage marker–positive cells by the total number of mononuclear cells isolated from the injured and non-injured spinal cord. For the flow cytometry analyses, the Fc receptors were initially blocked using anti-mouse CD16/32 (0.25 μg; eBioscience). Cells were then immunostained for 30 min at 4 °C using the specified antibodies (from BD Biosciences or eBioscience) (Rose et al., 2012; Getts et al., 2014; Edwards et al., 2017; Ifergan et al., 2017). Cells were acquired on a BD Canto II and analyzed using BD FACSDiva version 6.1 software.

2.6. Quantification of IMPs uptake by microglia and CD11b$^+$ splenocytes

CNS cells from naïve mice were isolated by Percoll gradient centrifugation from homogenized combined brain and spinal cords as previously described (Terry et al., 2016). CD11b$^+$ microglia were enriched using magnetic cell sorting (Miltenyi Biotec; Auburn, CA) according to the manufacturer's instructions. CD45^{int} CD11b$^+$ CD39$^+$ Ly6C$^-$ Ly6G$^-$ monocytes purity was >85% as assessed by flow cytometry. CD11b$^+$ splenocytes were also isolated from the same mice using magnetic cell sorting as well. Cells were counted, and plated in 96-well microtiter plates at a density of 1×10^5 cells/well for microglia and 1×10^6 cells/well for spleens in a total volume of 200 μl of R10 media (RPMI with 10% (volume/volume) fetal bovine serum (FBS), 2 mM L-glutamine, 100 U/ml penicillin, 100 μg/ml streptomycin). Cells were either left rested or activated for 24 h at 37 °C in presence of LPS (10 ng/ml) from *E. coli* serotype 0111:B4 (Sigma). Cells were then washed, and green-labeled IMPs (2.5 μg/ml) were added for 1 h at 37 °C. Flow cytometry analyses followed.

2.7. Western analyses

Mice were euthanized via CO_2 inhalation. A 1 mm region containing the spinal lesion was removed and lysed in Tissue Protein Extraction Reagent (T-PER) (Thermo Scientific) supplemented with 100× HALT protease inhibitor cocktail (Thermo Scientific) with mechanical disruption. Debris was removed by centrifugation for 5 min at 4 °C. Protein concentrations were determined by bicinchoninic acid (BCA) protein assay (Thermo Scientific) with a standard curve of bovine serum albumin. Cell lysates were mixed with reducing Laemmli loading buffer and separated by sodium dodecyl sulfate polyacrylamide gel electrophoresis (SDS-PAGE). Blots were transferred to Immobilon-P membranes (Millipore) and washed with TBS-T (0.1% Tween 20). Primary and secondary antibodies used are listed in Supplementary Table 1. Blots were developed using ECL Western Blotting Substrate (Thermo Scientific) and Amersham HyperFilm ECL (GE Healthcare). Membranes were stripped and re-probed using Restore Western Blot Stripping Buffer (Thermo Scientific). Western blot films were scanned using a CanoScan 9000F scanner (Canon) and the images quantified using the Analyze Gels tool in Fiji Is Just ImageJ (Fiji) (Schindelin et al., 2012).

2.8. Histology and immunohistochemistry

Mice were euthanized via CO_2 inhalation and transcardially perfused with ice cold PBS followed by 4% paraformaldehyde in PBS. Spinal cords were removed and post-fixed for 2 h in 4% PFA on ice. Samples were dehydrated overnight in 30% sucrose at 4 °C and then

embedded in O.C.T. matrix (Tissue-Tek). 16, 20, or 30 μm sagittal sections were cut on a Leica CM3050S cryostat and collected on microscope slides (Fisher Scientific Superfrost). Slides were washed in PBS-T (0.05% Triton X-100) and incubated with primary antibodies at 4 °C overnight in blocking media (5% normal goat serum in PBS-T). Primary and secondary antibodies used are listed in Supplementary Table 1. Stained sections were mounted in ProLong Gold (Molecular Probes). Images were acquired with a Leica SP5 AOBS confocal microscope. Large format images were stitched using the native Leica Application Suite — Advanced Fluorescence software.

2.9. Image quantification

Quantification of immunofluorescent images was performed by blinded investigators using the “Icy” bioimage software package (de Chaumont et al., 2012). Only mid-sagittal sections, identified by the presence of the ependymal canal, were used for image acquisition. When quantifying CS56 intensity, the lesion center was defined as the GFAP-area surrounded by a bright GFAP+ border. The lesion rim was defined as any spinal tissue outside of the lesion center but within 250 μm of the bright GFAP+ border that bounds the lesion center. These regions were outlined using Icy’s polygon ROI tool. Areas and signal intensities were automatically determined using Icy’s native ROI Statistics tool.

2.10. Statistical analyses

Data were analyzed using GraphPad Prism software (version 5.04), and statistical significance was assigned at a predetermined cutoff of $p < 0.05$. Comparisons between pairs of experimental groups were performed using Student’s *t*-test. Comparisons among three or more groups were conducted using ANOVA with Tukey’s Multiple Comparison post-hoc test or ANOVA with Bonferroni’s post-hoc test. Mouse BMS behavioral scores were compared between IMPs- and PBS-treated groups by two-way repeated measures ANOVA. All data are presented as mean ± standard error of the mean (SEM) unless otherwise noted.

3. Results

3.1. IMPs reduce inflammatory cell influx into the injured spinal cord without altering the number of microglia

To determine the effects of IMPs administration on cell infiltration into an injured mouse spinal cord, IMPs were given intravenously (iv) 2 h and 24 h after a severe contusion injury. The gating strategy is shown in Supplementary Fig. 1 (Rose et al., 2012; Getts et al., 2014; Edwards et al., 2017; Ifergan et al., 2017). The mice were sacrificed at 48 h post-SCI for flow cytometry analysis of cells in the lesion site. The total number of inflammatory cells, and in particular $CD45^{hi}$ $CD11b^{+}$ $Ly6G^{-}$ $CD11c^{+}$ myeloid dendritic cells (mDCs), $CD45^{hi}$ $CD11b^{+}$ $Ly6G^{-}$ $CD11c^{-}$ macrophages/monocytes, $CD45^{hi}$ $CD11b^{+}$ $Ly6G^{-}CD11c^{-}$ $Ly6C^{hi}$ inflammatory monocytes, $CD45^{hi}$ $CD11b^{+}$ $Ly6G^{-}CD11c^{-}$ $Ly6C^{lo}$ non-inflammatory monocytes, and $CD45^{hi}$ $CD11b^{-}CD4^{+}$ T cells, were all significantly reduced in the lesions of IMPs treated mice compared to vehicle treated controls (Supplementary Fig. 1 and Fig. 1). No effect was observed on $CD45^{hi}$ $CD11b^{+}$ $Ly6G^{+}$ neutrophils. Importantly, iv infusion of IMPs did not alter the number of microglia ($CD45^{int}$ $CD11b^{+}$ $Ly6C^{lo}$). No changes were observed in the spinal cord distal from the lesion (Supplementary Fig. 2) These observations

show that IMPs treatment reduces infiltration of blood-borne inflammatory cells into the injured spinal cord without altering the microglial population.

3.2. Reduction of M1 macrophages and microglial activation following IMPs treatment

We evaluated the profile of the macrophage population infiltrating the injured site of the spinal cord and observed a decrease in $CD86^+$ MHC II^+ M1 macrophages in the spinal cord of IMPs-treated mice compared to PBS treated mice (Fig. 2A). Along with the M1 decrease, IL-10^+ macrophages increased in IMPs-treated mice (Fig. 2A right panels), suggesting that in addition of reducing cell entry in the spinal cord, IMPs treatment shifted the profile of the infiltrating cells. Further, analysis of the microglial profile showed a large decrease in CD86 expression (Fig. 2B), while MHC II and IL-10 remained unchanged. To determine whether the microglial changes reflected direct uptake of particles by microglia or an indirect phenomenon caused by the reduction of cell infiltration and inflammation in the CNS, microglia were isolated and exposed to green labeled IMPs. Microglia were either left resting or activated 24 h with LPS prior to particle exposure. Neither resting nor activated microglia were able to uptake IMPs (Supplementary Fig. 3A), whereas $CD11b^+$ splenocytes had a high capacity to uptake the particles (Supplementary Fig. 3B). These data suggest that the reduction in CD86 expression on microglia might be due to a reduced inflammatory environment in the spinal cord.

To define changes in the inflammatory environment, we measured the content of cytokine and chemokine mRNAs in the lesion sites of spinal cords at 48 h post injury using a PCR array that contains 84 genes of interest. We observed that most genes tested were downregulated in IMPs treated mice (Fig. 2C), with 19 of these genes showing a significant reduction ($n = 5$ mice per group; Supplementary Table 2). Of interest, there were significant reductions in 7 chemokine genes, most notably *Ccl2, Ccl4* and *Ccl12*, that are chemoattractants for monocytes/macrophages and DCs, as well as *Ccl17*, which is a chemoattractant for T cells. The microarray analysis thus suggests that IMP treatment significantly ameliorated the pro-inflammatory environment in the injured spinal cord, providing a likely explanation for the reduction in microglial activation observed in these mice.

3.3. IMPs treatment attenuates chronic fibrotic scarring

After SCI, a fibrotic scar forms that is marked by an accumulation of fibronectin, fibroblasts, and other extracellular matrix (ECM) molecules such as collagen type IV, laminin, and tenascins (Goritz et al., 2011; Soderblom et al., 2013). To examine the effects of IMPs treatment on fibrotic scarring, mice were subjected to a severe SCI and treated with iv IMPs or PBS at 2, 24, and 48 h after injury (Fig. 3A). At 13 weeks post injury, the lesions in PBS treated animals displayed intense fibronectin immunostaining. In contrast, in IMPs treated animals the intensity of fibronectin immunostaining inside the lesion was significantly reduced. To quantify the immunostaining intensity of fibronectin, we computed mean intensity where the total staining intensity of fibronectin inside the lesion was divided by the lesion area (Fig. 3B and C, Supplementary Fig. 4A). Western blot analyses at 12 weeks post injury confirmed that IMPs treatment markedly reduced levels of fibronectin and collagen IV in the lesions (Fig. 3D, F–H). Importantly, levels of fibronectin remained significantly

elevated in vehicle treated mice at 10 months (41 weeks) post SCI, indicative of chronic fibrotic scarring, but were not significantly different from uninjured levels in IMPs-treated mice (Fig. 3E and F). Thus, limiting acute infiltration of hematogenous monocytes via IMPs treatment substantially reduced chronic fibrotic scarring after SCI.

3.4. IMPs treatment reduces deposition of chondroitin sulfate proteoglycans (CSPGs)

Mice subjected to a severe SCI were treated with either iv PBS or IMPs and examined at various times thereafter for levels of CSPGs in the injured sites. At 13 weeks post injury, PBS treated animals showed intense immunostaining for CSPGs (anti-CS-56 antibody) in the lesion core as well as in the $GFAP^+$ lesion rim immediately surrounding the lesion site (Fig. 4A). The immunostaining of CS-56 was quantified using the same mean intensity method used for quantifying fibronectin as described above. IMPs treatment significantly reduced accumulation of CSPGs both in the lesion sites and in the GFAP+ lesion rims (Fig. 4B, Supplementary Fig. 4B). Similarly, IMPs treatment reduced levels of neurocan at 12 weeks post injury, and levels of neurocan remained significantly decreased at 10 months (41 weeks) post injury (data not shown). Moreover, at 10 months post injury the IMPs treated group also had significantly decreased levels of tenascin-R (Fig. 4C), which has been shown to inhibit axonal outgrowth, but no reduction in tenascin-C or laminin, which are permissive for axon growth (Anderson et al., 2016) (Fig. 4D–F). Thus inhibiting infiltration of hMΦ by IMPs infusion resulted in a milieu in the injured spinal cord that is more permissive to axonal outgrowth and regeneration.

3.5. IMPs treatment does not alter glial scarring, lesion size, or demyelination

We next evaluated the effects of IMPs treatment on glial scarring by quantifying the mean intensity of GFAP and vimentin immunostaining within the lesion rim at various time points ranging from 7 to 90 days post-injury in IMPs and PBS treated mice. There were no differences between the IMPs and vehicle treated groups in either GFAP or vimentin immunostaining at any of the time points assessed (Fig. 5A–D). Further, immunoblotting analyses at 41 weeks post injury also showed no difference between the groups in levels of GFAP (Fig. 5E and F). We also quantified chronic lesion size at six months (26 weeks) post-injury. Two dimensional lesion areas were measured from three to four midsagittal sections from each mouse. Interestingly, we observed no difference in lesion size between IMPs and vehicle treated groups (Supplementary Fig. 4C) Our findings thus implicate early-infiltrating hematogenous monocytes as highly selective contributors to fibrosis that do not play indispensable roles in gliosis or lesion size after SCI.

In order to determine whether IMPs treatment alters apoptosis subacutely after SCI we quantified the number of cleaved caspase-3 positive cells present in the lesioned spinal cord using immunohistochemistry. At 7 days post SCI, we found no difference in the number of cleaved caspase-3 positive cells between the IMPs and PBS treated groups (data not shown). We also measured myelin sparing at 7 days post SCI using FluoroMyelin stained sections to quantify myelin content. Both IMP and PBS treated animals displayed significant demyelination around the lesion site. However, no significant differences in myelin sparing were found between the treatment groups at 7 days post injury (Supplementary Fig. 5 A and B).

3.6. IMPs treatment results in higher axon densities in chronically injured spinal cords

Since our observations suggested that IMPs infusion leads to a microenvironment more conducive to axonal regeneration or sparing, we evaluated axon density in the spinal cord at 6 months (26 weeks) post injury. To visualize axons, 30 μm thick mid-sagittal sections of injured spinal cords from PBS or IMPs treated animals were immunostained with SMI-312, a pan-axonal neurofilament marker (Fig. 6A, B) that has previously been used to visualize and quantify axons in the injured rodent spinal cord (Sahni et al., 2010; Sharp et al., 2014; Steward et al., 2014). IMPs treatment significantly increased SMI-312 neurofilament staining from 250 μm caudal up to 1500 μm caudal to the lesion site compared to PBS controls (Fig. 6C). Axon density in the lesion site itself trended higher with an almost twofold increase in IMPs treated animals compared to PBS-treated controls.

Serotonin (5-HT) is an important modulator of the central pattern generator and promotes stepping after SCI (Schmidt and Jordan, 2000). To examine the density of serotonergic fibers in and around the lesion after SCI, longitudinal sections of spinal cord 1 week and 13 weeks post SCI were immunostained for serotonin, and the number of serotonin^{+} fibers was quantified along the rostrocaudal axis of the spinal cord. We observed no difference in serotonergic fiber density between treatment groups at 1 week post SCI (data not shown). By contrast, at 13 weeks post injury we found a greater number of serotonergic fibers both within and rostral to the lesion in IMPs treated mice, suggesting sprouting of fibers. The number of serotonergic fibers did not differ significantly caudal to the lesion (Fig. 6D–F).

3.7. IMPs treatment significantly improves motor recovery after SCI

After a severe contusion SCI (100 kdyn, 60 s dwell time), mice were treated with either PBS or IMPs at 2, 24, and 48 h post injury followed by weekly assessments of locomotion using the Basso Mouse Scale (BMS) open field scoring method (Basso et al., 2006). Immediately after injury, there was no detectable difference between the IMPs-treated and PBS-control groups. At 6 weeks post injury and thereafter the treated group demonstrated significant and sustained behavioral improvement compared to control. Notably, at 11 weeks after injury the IMPs treated group showed a mean BMS score of 2.24 while the control group remained at the mean score of 1.04 (Fig. 7A). Detailed behavioral data showing BMS score distributions and recovery thresholds are shown in (Supplementary Fig. 6A–C).

We also examined the effects of IMPs treatment on behavioral recovery in mice subjected to a more moderate contusion SCI (60 kdyn, 0 s dwell time). Mice were treated with IMPs or PBS iv at 2, 24, and 48 h post injury and assessed weekly using the BMS. At 8 weeks post injury and thereafter, the IMPs treated group significantly outperformed the control group (Fig. 7B). At week 12, the IMPs treated mice had a mean BMS score of 6.33 while the PBS treated mice remained at a score of 4.40 (Fig. 7B). Detailed behavioral data from this moderate injury experiment are displayed in (Supplementary Fig. 6D–F).

4. Discussion

The rapid influx of immune cells into an injured spinal cord contributes to a cascade of secondary injury processes that lead to further axonal damage, cell death, demyelination and

fibrosis and reactive gliosis with scar formation (Popovich et al., 1999; Fleming et al., 2006; Donnelly and Popovich, 2008; Evans et al., 2014; Zhu et al., 2015a). Systemic depression of monocytes and/or macrophages through administration of liposome-encapsulated clodronate (Popovich et al., 1999; Zhu et al., 2015a), dehydroepiandrosterone (Fiore et al., 2004), minocycline (Stirling et al., 2004), FK506 (Lopez-Vales et al., 2005), or antibody to alphaD (Mabon et al., 2000) improves tissue repair and enhances functional recovery after SCI. However, other studies have also demonstrated that macrophages clear cellular debris and secrete neurotrophic factors and anti-inflammatory cytokines to support axonal regeneration (Yin et al., 2003; Hashimoto et al., 2005; Bouhy et al., 2006; Shechter et al., 2013), and systemic depression of macrophages reduces remyelination after SCI (Kotter et al., 2005). These seemingly contradictory roles of macrophages in the injured spinal cord highlight the complex nature of the inflammatory responses after SCI and argue for the need for treatments that selectively ablate deleterious subpopulations of macrophages while preserving beneficial ones.

Although both hematogenous monocytes and microglia differentiate into macrophages in the injured spinal cord, recent evidence suggests that hMΦ, but not mMΦ, are primarily responsible for secondary axonal dieback after SCI (Durafourt et al., 2012; Evans et al., 2014; Gensel and Zhang, 2015). Hence, targeting the early influx of hematogenous monocytes but not microglia or other populations of immune regulatory cells, might improve tissue repair and functional recovery after SCI. However, to date, selectively inhibiting early infiltration of hematogenous monocytes into lesions has been challenging because they are not easily distinguishable from resident microglia.

Intravenously injected IMPs bind to the scavenger receptor MARCO expressed on bone marrow derived monocytes and induce the sequestration and apoptosis of hΦM in the spleen (Getts et al., 2012; Getts et al., 2014). IMPs treatment thus targets circulating monocytes/macrophages that can gain rapid access to the injured CNS. Significantly, we showed that IMPs do not bind to microglia or alter the number of microglia after SCI. Our data suggest that IMPs may be more advantageous for treating SCI than previously described approaches that are not as specific for hΦM. Moreover, the nanoparticles are made of an FDA-approved material that is immunologically inert, stable at room temperature and could be given easily immediately after SCI by emergency medical technicians at an accident site, or by a rapid response team in the emergency room, to prevent secondary damage, thereby improving outcome. IMPs are thus a highly translatable potential clinical tool for treating acute SCI.

Interestingly, our data indicate that there is no uptake of IMPs by microglia, which thus protects those cells from any potential action of the particles. Prior studies have indicated a lack of MARCO expression on microglia (Hickman et al., 2013; Zhang et al., 2014), reinforcing the importance of this scavenger receptor in the engulfment of IMPs by hematogenous monocytes. However, IMPs treatment does indirectly affect microglial activation. Microglia displayed a decreased activation profile following IMPs treatment. This decreased activation profile could be the result of a less inflammatory lesion environment acting upon local microglia or of impaired trafficking of M1 macrophages into the injury site. In addition, we observed a reduction in $CD4^+$ T lymphocytes presence in lesions of IMPs treated mice. Since T lymphocytes are not competent to uptake molecules and do not

express MARCO, we propose that the reduction of chemokine expression following IMPs injection attracts less lymphocytes to the lesion site, while the decrease of competent antigen presenting cells (monocytes, macrophages and mDCs) also reduces the ability of T lymphocytes to become activated and to proliferate at the lesion site.

In this study, we observed significantly reduced chronic fibrotic scarring after IMPs treatment, as evidenced by decreased levels of fibronectin and collagen IV, for up to 10 months post injury. After SCI, fibronectins are secreted as a soluble dimer formed primarily by Col1α1+/PDGFR-β+/CD13+ perivascular fibroblasts and GLAST+ type A pericytes starting three days post-injury (Goritz et al., 2011; Soderblom et al., 2013). Soluble fibronectin dimers bind to integrins, mainly α5β1 integrin, and this interaction leads to a conformation change of fibronectin that exposes its intramolecular binding regions (Pytela et al., 1985; Berton and Lowell, 1999; To and Midwood, 2011). This process initiates assembly of fibronectin dimers into a dense, insoluble, fibrilar meshwork, or matrix, that forms the chronic fibrotic scar (Stoffels et al., 2013; Zhu et al., 2015b). Since hematogenous monocytes and hMΦ highly express α5β1 integrins on their surface, it seemed likely that they mediate fibronectin fibril formation after SCI. However, we quantified the amount of insoluble fibronectin matrix at 7 days post SCI using a DOC digest technique (Zhu et al., 2015b) and observed no difference in insoluble matrix-assembled fibronectin, or total fibronectin levels, in IMPs treated mice compared to controls (Supplementary Fig. 7). This suggests that inhibiting the early influx of hematogenous monocytes does not decrease chronic fibrotic scarring by reducing direct macrophage effects on fibronectin fibril assembly. However, macrophages also create a pro-fibrotic milieu in many organs by secreting TGF-β and other pro-fibrotic cytokines including PDGF and IL-1 that activate fibroblasts to produce connective tissue growth factor (CTGF) and collagen IV via both SMAD2/3 dependent and independent pathways (Friedman, 2003; Leask and Abraham, 2004; Wynn and Barron, 2010). The reduced levels of inflammatory cytokines after IMPs treatment, as well as the parallel reductions in collagen IV and fibronectin, suggest that the reduction in fibrotic scarring may reflect the decrease in cytokine production. However, hematogenous monocytes and hMΦ recruit perivascular fibroblasts into spinal lesions, and deleting hematogenous macrophages reduces fibroblast accumulation at 7 and 14 days after SCI (Zhu et al., 2015a). It is therefore possible that IMPs treatment also alters the migration of fibroblasts into the lesion thereby reducing fibronectin accumulation.

IMPs treatment reduced levels of CSPGs, marked by CS-56 and neurocan antibodies, in injured sites up to 10 months after SCI. CSPGs are highly inhibitory to neurite outgrowth (Margolis et al., 1996; Inatani et al., 2001). Decreased CSPG accumulation following IMPs treatment may be directly attributed to the reduced number of macrophages, which synthesize CSPGs (Jones et al., 2002; David and Kroner, 2011). However, since fibronectin binds the glycosaminoglycan chain of CSPGs (Perkins et al., 1979) CSPG levels may also be attenuated because of the reduction in fibrotic scarring. At 10 months post injury the IMPs treated group also had significantly decreased levels of tenascin-R, which inhibits axonal outgrowth, without any reduction in tenascin-C or laminin, which are permissive for axon growth (Anderson et al., 2016) (Fig. 4C–F). Thus, IMPs infusion resulted in a milieu within the injured spinal cord that is more permissive to axon outgrowth and regeneration.

Notably, we did not observe changes in GFAP or vimentin accumulation in the lesion after IMPs treatment either acutely or chronically. Our findings thus implicate early-infiltrating hematogenous monocytes as highly selective contributors to fibrosis that do not play an indispensable role in gliosis after SCI. The reduction in CSPGs without any apparent change in gliosis suggests that astrocytes are not the main source of the CSPGs, consistent with a recent study showing that ablation of reactive astrocytes after SCI does not reduce levels of aggrecan (Anderson et al., 2016). Moreover, we show that reduced fibrotic scarring, independent from altered glial scarring, significantly improves behavioral outcomes. This suggests that reduction in fibrotic scarring will be an important element of therapeutic approaches to SCI.

IMPs treatment increased the number of axons immunostained for neurofilament (SMI-312) caudal to the lesion and the number of serotonergic fibers rostral to the lesion. Neurofilament staining cannot differentiate between spared and regenerating axons, and this result could be interpreted either as an increase in the number of preserved axons or an enhancement of axonal growth and regeneration. However, serotonergic fiber staining showed no difference between groups at one week post injury but significant differences at 13 weeks, suggesting that IMPs treatment may enhance late fiber sprouting.

To enhance the translational relevance of our study, we began treating our animals with IMPs at 2 h post-SCI. We consider this a rapid yet clinically achievable time point for IMPs administration. We chose to use a particularly severe injury as our primary model since any new therapy for SCI will likely be tested first in ASIA A patients. However, in view of the lack of any apparent toxicity, IMPs therapy may also be helpful for patients with less severe injuries. We therefore modeled a less severe injury and similarly found a significant improvement in motor function. Thus, IMPs could potentially be an intervention for all patients with a significant acute SCI. The nanoparticles are stable at room temperature and easily could be given immediately after SCI by first responders at the site of an accident or in the emergency room to prevent secondary damage, thereby significantly improving outcome.

In summary, our findings support the idea that the early-infiltrating hematogenous monocytes contribute to neuroinflammatory damage and fibrotic scar formation after SCI. Moreover, IMPs may provide a practical and easily translatable means of improving outcome after SCI.

Supplementary Material

Refer to Web version on PubMed Central for supplementary material.

Acknowledgments

We thank Dr. Vytas Bindokas (Integrated Light Microcopy Core Facility, University of Chicago) for sharing his expertise with us.

Funding

This research was supported by EB013198 and NS026543 (to S.D.M), and F30NS093811 (to J.G.C).

References

Anderson MA, Burda JE, Ren Y, Ao Y, O'Shea TM, Kawaguchi R, et al. Astrocyte scar formation aids central nervous system axon regeneration. Nature. 2016; 532(7598):195–200. [PubMed: 27027288]

Basso DM, Fisher LC, Anderson AJ, Jakeman LB, McTigue DM, Popovich PG. Basso Mouse Scale for locomotion detects differences in recovery after spinal cord injury in five common mouse strains. J Neurotrauma. 2006; 23(5):635–659. [PubMed: 16689667]

Beck KD, Nguyen HX, Galvan MD, Salazar DL, Woodruff TM, Anderson AJ. Quantitative analysis of cellular inflammation after traumatic spinal cord injury: evidence for a multiphasic inflammatory response in the acute to chronic environment. Brain. 2010; 133(Pt 2):433–447. [PubMed: 20085927]

Berton G, Lowell CA. Integrin signalling in neutrophils and macrophages. Cell Signal. 1999; 11(9): 621–635. [PubMed: 10530871]

Boros P, Ochando JC, Chen SH, Bromberg JS. Myeloid-derived suppressor cells: natural regulators for transplant tolerance. Hum Immunol. 2010; 71(11):1061–1066. [PubMed: 20705113]

Bouhy D, Malgrange B, Multon S, Poirrier AL, Scholtes F, Schoenen J, et al. Delayed GM-CSF treatment stimulates axonal regeneration and functional recovery in paraplegic rats via an increased BDNF expression by endogenous macrophages. FASEB J. 2006; 20(8):1239–1241. [PubMed: 16636109]

Bush TG, Puvanachandra N, Horner CH, Polito A, Ostenfeld T, Svendsen CN, et al. Leukocyte infiltration, neuronal degeneration, and neurite outgrowth after ablation of scar-forming, reactive astrocytes in adult transgenic mice. Neuron. 1999; 23(2):297–308. [PubMed: 10399936]

de Chaumont F, Dallongeville S, Chenouard N, Herve N, Pop S, Provoost T, et al. Icy: an open bioimage informatics platform for extended reproducible research. Nat Methods. 2012; 9(7):690–696. [PubMed: 22743774]

David S, Kroner A. Repertoire of microglial and macrophage responses after spinal cord injury. Nat Rev Neurosci. 2011; 12(7):388–399. [PubMed: 21673720]

Donnelly DJ, Popovich PG. Inflammation and its role in neuroprotection, axonal regeneration and functional recovery after spinal cord injury. Exp Neurol. 2008; 209(2):378–388. [PubMed: 17662717]

Durafourt BA, Moore CS, Zammit DA, Johnson TA, Zaguia F, Guiot MC, et al. Comparison of polarization properties of human adult microglia and blood-derived macrophages. Glia. 2012; 60(5):717–727. [PubMed: 22290798]

Edwards RG, Kopp SJ, Ifergan I, Shui JW, Kronenberg M, Miller SD, et al. Murine corneal inflammation and nerve damage after infection with HSV-1 are promoted by HVEM and ameliorated by immune-modifying nanoparticle therapy. Invest Ophthalmol Vis Sci. 2017; 58(1): 282–291. [PubMed: 28114589]

Estrada V, Brazda N, Schmitz C, Heller S, Blazyca H, Martini R, et al. Long-lasting significant functional improvement in chronic severe spinal cord injury following scar resection and polyethylene glycol implantation. Neurobiol Dis. 2014; 67:165–179. [PubMed: 24713436]

Evans TA, Barkauskas DS, Myers JT, Hare EG, You JQ, Ransohoff RM, et al. High-resolution intravital imaging reveals that blood-derived macrophages but not resident microglia facilitate secondary axonal dieback in traumatic spinal cord injury. Exp Neurol. 2014; 254:109–120. [PubMed: 24468477]

Faulkner JR, Herrmann JE, Woo MJ, Tansey KE, Doan NB, Sofroniew MV. Reactive astrocytes protect tissue and preserve function after spinal cord injury. J Neurosci. 2004; 24(9):2143–2155. [PubMed: 14999065]

Fiore C, Inman DM, Hirose S, Noble LJ, Igarashi T, Compagnone NA. Treatment with the neurosteroid dehydroepiandrosterone promotes recovery of motor behavior after moderate contusive spinal cord injury in the mouse. J Neurosci Res. 2004; 75(3):391–400. [PubMed: 14743452]

Flaishon L, Becker-Herman S, Hart G, Levo Y, Kuziel WA, Shachar I. Expression of the chemokine receptor CCR2 on immature B cells negatively regulates their cytoskeletal rearrangement and migration. Blood. 2004; 104(4):933–941. [PubMed: 15126315]

Fleming JC, Norenberg MD, Ramsay DA, Dekaban GA, Marcillo AE, Saenz AD, et al. The cellular inflammatory response in human spinal cords after injury. Brain. 2006; 129(Pt 12):3249–3269. [PubMed: 17071951]

Friedman SL. Liver fibrosis — from bench to bedside. J Hepatol. 2003; 38(Suppl 1):S38–53. [PubMed: 12591185]

Gensel JC, Zhang B. Macrophage activation and its role in repair and pathology after spinal cord injury. Brain Res. 2015

Getts DR, Martin AJ, McCarthy DP, Terry RL, Hunter ZN, Yap WT, et al. Microparticles bearing encephalitogenic peptides induce T-cell tolerance and ameliorate experimental autoimmune encephalomyelitis. Nat Biotechnol. 2012; 30(12):1217–1224. [PubMed: 23159881]

Getts DR, Terry RL, Getts MT, Deffrasnes C, Muller M, van Vreden C, et al. Therapeutic inflammatory monocyte modulation using immune-modifying microparticles. Sci Transl Med. 2014; 6(219):219ra7.

Goritz C, Dias DO, Tomilin N, Barbacid M, Shupliakov O, Frisen J. A pericyte origin of spinal cord scar tissue. Science. 2011; 333(6039):238–242. [PubMed: 21737741]

Grosso MJ, Matheus V, Clark M, van Rooijen N, Iannotti CA, Steinmetz MP. Effects of an immunomodulatory therapy and chondroitinase after spinal cord hemisection injury. Neurosurgery. 2014; 75(4):461–471. [PubMed: 24871142]

Hashimoto M, Nitta A, Fukumitsu H, Nomoto H, Shen L, Furukawa S. Inflammation-induced GDNF improves locomotor function after spinal cord injury. Neuroreport. 2005; 16(2):99–102. [PubMed: 15671854]

Hickman SE, Kingery ND, Ohsumi TK, Borowsky ML, Wang LC, Means TK, El Khoury J. The microglial sensome revealed by direct RNA sequencing. Nat Neurosci. 2013; 16(12):1896–1905. [PubMed: 24162652]

Horn KP, Busch SA, Hawthorne AL, van Rooijen N, Silver J. Another barrier to regeneration in the CNS: activated macrophages induce extensive retraction of dystrophic axons through direct physical interactions. J Neurosci. 2008; 28(38):9330–9341. [PubMed: 18799667]

Ifergan I, Davidson TS, Kebir H, Xu D, Palacios-Macapagal D, Cann J, et al. Targeting the GM-CSF receptor for the treatment of CNS autoimmunity. J Autoimmun. 2017

Inatani M, Honjo M, Otori Y, Oohira A, Kido N, Tano Y, et al. Inhibitory effects of neurocan and phosphacan on neurite outgrowth from retinal ganglion cells in culture. Invest Ophthalmol Vis Sci. 2001; 42(8):1930–1938. [PubMed: 11431463]

Jones LL, Yamaguchi Y, Stallcup WB, Tuszynski MH. NG2 is a major chondroitin sulfate proteoglycan produced after spinal cord injury and is expressed by macrophages and oligodendrocyte progenitors. J Neurosci. 2002; 22(7):2792–2803. [PubMed: 11923444]

Jung H, Bhangoo S, Banisadr G, Freitag C, Ren D, White FA, et al. Visualization of chemokine receptor activation in transgenic mice reveals peripheral activation of CCR2 receptors in states of neuropathic pain. J Neurosci. 2009; 29(25):8051–8062. [PubMed: 19553445]

Kang YS, Cha JJ, Hyun YY, Cha DR. Novel C-C chemokine receptor 2 antagonists in metabolic disease: a review of recent developments. Expert Opin Investig Drugs. 2011; 20(6):745–756.

Kilkenny C, Browne WJ, Cuthill IC, Emerson M, Altman DG. Improving bioscience research reporting: the ARRIVE guidelines for reporting animal research. PLoS Biol. 2010; 8(6):e1000412. [PubMed: 20613859]

Kotter MR, Zhao C, van Rooijen N, Franklin RJ. Macrophage-depletion induced impairment of experimental CNS remyelination is associated with a reduced oligodendrocyte progenitor cell response and altered growth factor expression. Neurobiol Dis. 2005; 18(1):166–175. [PubMed: 15649707]

Kumamaru H, Saiwai H, Kobayakawa K, Kubota K, van Rooijen N, Inoue K, et al. Liposomal clodronate selectively eliminates microglia from primary astrocyte cultures. J Neuroinflammation. 2012; 9:116. [PubMed: 22651847]

Leask A, Abraham DJ. TGF-beta signaling and the fibrotic response. FASEB J. 2004; 18(7):816–827. [PubMed: 15117886]

Lemmon VP, Ferguson AR, Popovich PG, Xu XM, Snow DM, Igarashi M, et al. Minimum information about a spinal cord injury experiment: a proposed reporting standard for spinal cord injury experiments. J Neurotrauma. 2014; 31(15):1354–1361. [PubMed: 24870067]

Letellier E, Kumar S, Sancho-Martinez I, Krauth S, Funke-Kaiser A, Laudenklos S, et al. CD95-ligand on peripheral myeloid cells activates Syk kinase to trigger their recruitment to the inflammatory site. Immunity. 2010; 32(2):240–252. [PubMed: 20153221]

Leuschner F, Dutta P, Gorbatov R, Novobrantseva TI, Donahoe JS, Courties G, et al. Therapeutic siRNA silencing in inflammatory monocytes in mice. Nat Biotechnol. 2011; 29(11):1005–1010. [PubMed: 21983520]

Lopez-Vales R, Garcia-Alias G, Fores J, Udina E, Gold BG, Navarro X, et al. FK 506 reduces tissue damage and prevents functional deficit after spinal cord injury in the rat. J Neurosci Res. 2005; 81(6):827–836. [PubMed: 16041804]

Mabon PJ, Weaver LC, Dekaban GA. Inhibition of monocyte/macrophage migration to a spinal cord injury site by an antibody to the integrin alphaD: a potential new anti-inflammatory treatment. Exp Neurol. 2000; 166(1):52–64. [PubMed: 11031083]

Mack M, Cihak J, Simonis C, Luckow B, Proudfoot AE, Plachy J, et al. Expression and characterization of the chemokine receptors CCR2 and CCR5 in mice. J Immunol. 2001; 166(7): 4697–4704. [PubMed: 11254730]

Majed HH, Chandran S, Niclou SP, Nicholas RS, Wilkins A, Wing MG, et al. A novel role for Sema3A in neuroprotection from injury mediated by activated microglia. J Neurosci. 2006; 26(6): 1730–1738. [PubMed: 16467521]

Margolis RK, Rauch U, Maurel P, Margolis RU. Neurocan and phosphacan: two major nervous tissue-specific chondroitin sulfate proteoglycans. Perspect Dev Neurobiol. 1996; 3(4):273–290. [PubMed: 9117260]

Meda L, Cassatella MA, Szendrei GI, Otvos L Jr, Baron P, Villalba M, et al. Activation of microglial cells by beta-amyloid protein and interferon-gamma. Nature. 1995; 374(6523):647–650. [PubMed: 7715705]

Mizutani M, Pino PA, Saederup N, Charo IF, Ransohoff RM, Cardona AE. The fractalkine receptor but not CCR2 is present on microglia from embryonic development throughout adulthood. J Immunol. 2012; 188(1):29–36. [PubMed: 22079990]

Perkins ME, Ji TH, Hynes RO. Cross-linking of fibronectin to sulfated proteoglycans at the cell surface. Cell. 1979; 16(4):941–952. [PubMed: 222472]

Plemel JR, Wee Yong V, Stirling DP. Immune modulatory therapies for spinal cord injury—past, present and future. Exp Neurol. 2014; 258:91–104. [PubMed: 25017890]

Popovich PG, Guan Z, Wei P, Huitinga I, van Rooijen N, Stokes BT. Depletion of hematogenous macrophages promotes partial hindlimb recovery and neuroanatomical repair after experimental spinal cord injury. Exp Neurol. 1999; 158(2):351–365. [PubMed: 10415142]

Popovich PG, Guan Z, McGaughy V, Fisher L, Hickey WF, Basso DM. The neuropathological and behavioral consequences of intraspinal microglial/macrophage activation. J Neuropathol Exp Neurol. 2002; 61(7):623–633. [PubMed: 12125741]

Pytela R, Pierschbacher MD, Ruoslahti E. Identification and isolation of a 140 kd cell surface glycoprotein with properties expected of a fibronectin receptor. Cell. 1985; 40(1):191–198. [PubMed: 3155652]

Rose S, Misharin A, Perlman H. A novel Ly6C/Ly6G-based strategy to analyze the mouse splenic myeloid compartment. Cytometry A. 2012; 81(4):343–350. [PubMed: 22213571]

Sahni V, Mukhopadhyay A, Tysseling V, Hebert A, Birch D, McGuire TL, et al. BMPR1a and BMPR1b signaling exert opposing effects on gliosis after spinal cord injury. J Neurosci. 2010; 30(5):1839–1855. [PubMed: 20130193]

Sanae Kanno AF, Hirano Seishiro. A murine scavenger receptor MARCO recognizes polystyrene nanoparticles. Toxicol Sci. 2007; 97(2):398–406. [PubMed: 17361018]

Schindelin J, Arganda-Carreras I, Frise E, Kaynig V, Longair M, Pietzsch T, et al. Fiji: an open-source platform for biological-image analysis. Nat Methods. 2012; 9(7):676–682. [PubMed: 22743772]

Schmidt BJ, Jordan LM. The role of serotonin in reflex modulation and locomotor rhythm production in the mammalian spinal cord. Brain Res Bull. 2000; 53(5):689–710. [PubMed: 11165804]

Shantsila E, Wrigley B, Tapp L, Apostolakis S, Montoro-Garcia S, Drayson MT, et al. Immunophenotypic characterization of human monocyte subsets: possible implications for cardiovascular disease pathophysiology. J Thromb Haemost. 2011; 9(5):1056–1066. [PubMed: 21342432]

Sharp KG, Yee KM, Steward O. A re-assessment of long distance growth and connectivity of neural stem cells after severe spinal cord injury. Exp Neurol. 2014; 257:186–204. [PubMed: 24747827]

Shechter R, Miller O, Yovel G, Rosenzweig N, London A, Ruckh J, et al. Recruitment of beneficial M2 macrophages to injured spinal cord is orchestrated by remote brain choroid plexus. Immunity. 2013; 38(3):555–569. [PubMed: 23477737]

Soderblom C, Luo X, Blumenthal E, Bray E, Lyapichev K, Ramos J, et al. Perivascular fibroblasts form the fibrotic scar after contusive spinal cord injury. J Neurosci. 2013; 33(34):13882–13887. [PubMed: 23966707]

Steward O, Sharp KG, Yee KM, Hatch MN, Bonner JF. Characterization of ectopic colonies that form in widespread areas of the nervous system with neural stem cell transplants into the site of a severe spinal cord injury. J Neurosci. 2014; 34(42):14013–14021. [PubMed: 25319698]

Stirling DP, Khodarahmi K, Liu J, McPhail LT, McBride CB, Steeves JD, et al. Minocycline treatment reduces delayed oligodendrocyte death, attenuates axonal dieback, and improves functional outcome after spinal cord injury. J Neurosci. 2004; 24(9):2182–2190. [PubMed: 14999069]

Stoffels JM, de Jonge JC, Stancic M, Nomden A, van Strien ME, Ma D, et al. Fibronectin aggregation in multiple sclerosis lesions impairs remyelination. Brain. 2013; 136(Pt 1):116–131. [PubMed: 23365094]

Terry RL, Ifergan I, Miller SD. Experimental autoimmune encephalomyelitis in mice. Methods Mol Biol. 2016; 1304:145–160. [PubMed: 25005074]

To WS, Midwood KS. Plasma and cellular fibr onectin: distinct and independent functions during tissue repair. Fibrogenesis Tissue Repair. 2011; 4:21. [PubMed: 21923916]

Wynn TA, Barron L. Macrophages: master regulators of inflammation and fibrosis. Semin Liver Dis. 2010; 30(3):245–257. [PubMed: 20665377]

Yin Y, Cui Q, Li Y, Irwin N, Fischer D, Harvey AR, et al. Macrophage-derived factors stimulate optic nerve regeneration. J Neurosci. 2003; 23(6):2284–2293. [PubMed: 12657687]

Zhang Y, Chen K, Sloan SA, Bennett ML, Scholze AR, O'Keeffe S, Phatnani HP, Guarnieri P, Caneda C, Ruderisch N, Deng S, Liddelow SA, Zhang C, Daneman R, Maniatis T, Barres BA, Wu JQ. An RNA-sequencing transcriptome and splicing database of glia, neurons, and vascular cells of the cerebral cortex. J Neurosci. 2014; 34(36):11929–11947. [PubMed: 25186741]

Zhu Y, Soderblom C, Krishnan V, Ashbaugh J, Bethea JR, Lee JK. Hematogenous macrophage depletion reduces the fibrotic scar and increases axonal growth after spinal cord injury. Neurobiol Dis. 2015a; 74:114–125. [PubMed: 25461258]

Zhu Y, Soderblom C, Trojanowsky M, Lee DH, Lee JK. Fibronectin matrix assembly after spinal cord injury. J Neurotrauma. 2015b; 32(15):1158–1167. [PubMed: 25492623]

Appendix A. Supplementary data

Supplementary data to this article can be found online at http://dx.doi.org/10.1016/j.nbd.2017.08.006.

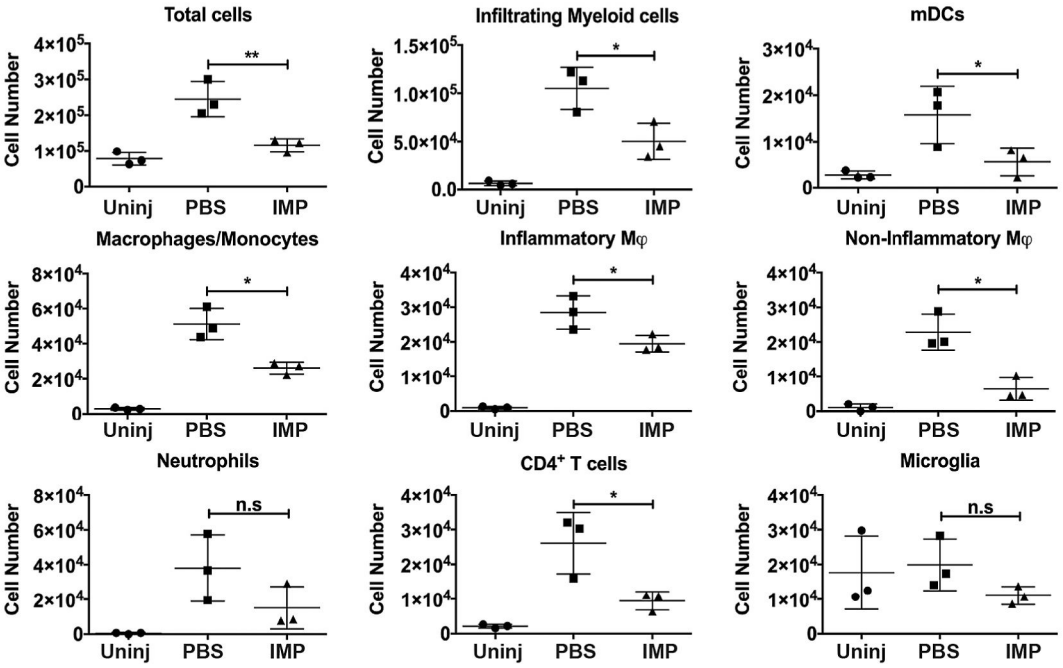

Fig. 1.

Treatment with IMPs reduces influx of inflammatory cells into the lesion after SCI. Mice received IMPs (black bars) or vehicle (PBS; grey bars) 2 h and 24 h after a SCI and were sacrificed at 48 h to analyze the extent of peripheral cell infiltration at the site of the injury. Uninjured control mice (white bars) also were analyzed. Cells within the lesion were counted and their profiles evaluated by FACS. IMPs treatment did not alter the number of microglia ($CD45^{int}$ $CD11b^{+}$ LyC^{lo}) but significantly reduced the influx of dendritic cells ($CD45^{hi}$ $CD11b^{+}$ $Ly6G^{-}$ $CD11c^{+}$), macrophages/monocytes ($CD45^{hi}$ $CD11b^{+}$ $Ly6G^{-}$ $CD11c^{-}$), inflammatory monocytes (inflammatory φ; $CD45^{+}$ $CD11b^{+}$ $Ly6G^{-}$ $CD11c^{-}$ $Ly6c^{hi}$), non-inflammatory monocytes (non-inflammatory φ; $CD45^{+}$ $CD11b^{+}$ $Ly6G^{-}$ $CD11c^{-}$ $Ly6c^{lo}$) and $CD4^{+}$ T cells ($CD45^{hi}$ $CD11b^{-}$ $CD4^{+}$). No significant difference was observed on neutrophils ($CD45^{+}$ $CD11b^{+}$ $Ly6G^{+}$). Values are the means of 3 independent experiments (n = 4–6 mice per experiment). All data are presented as mean ± SEM. Groups were compared by ANOVA followed by Tukey's multiple comparison test. *$p < 0.05$, **$p < 0.01$.

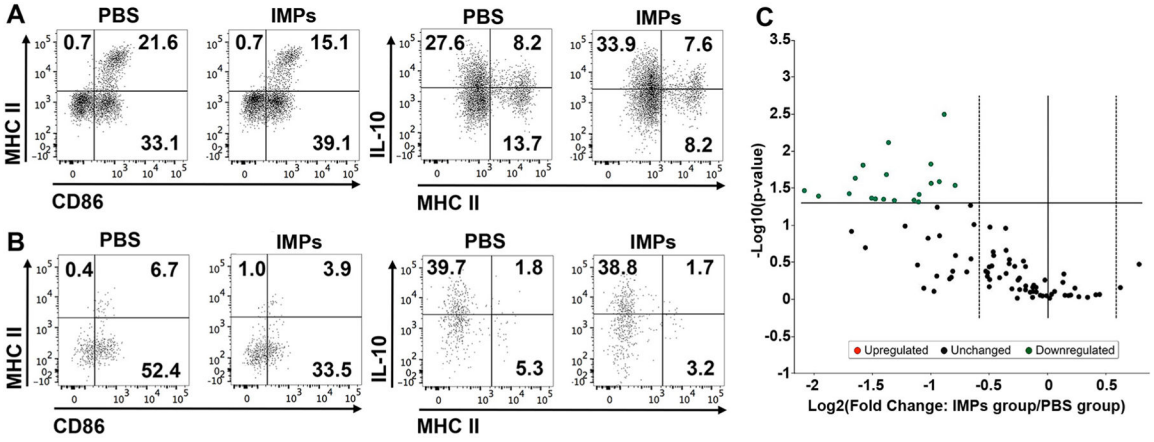

Fig. 2.

IMPs treatment reduces M1 macrophage and microglia activation in the lesions of SCI mice. Mice received IMPs or vehicle 2 h and 24 h after a SCI and were sacrificed at 48 h to (A) analyze the macrophage profile of infiltrating cells, (B) evaluate the microglia profile and (C) quantify the chemokines and cytokines in the injured part of the CNS. (A and B) Macrophages ($CD45^{hi}$ $CD11b^{+}$ $Ly6G^{-}$ $CD11c^{-}$) show a reduced M1 profile ($MHCII^{+}$ $CD86^{+}$) along with increased IL-10 expression in mice treated with IMPs. In the same mice, microglia ($CD45^{int}$ $CD11b^{+}$ LyC^{lo}) had reduced expression of the costimulatory molecule CD86. Data shown are representative of $n = 2$ independent experiments with 5–6 mice pooled for each experiment. (C) Volcano plot for differential gene expression showing statistical significance vs. fold change. Each point represents the results of one gene in which the x-axis is the log 2 fold change for the ratio IMPs treated mice vs PBS treated mice, whereas the y-axis is the −Log10 of *p*-value. Vertical dash lines represent differential expression differences of ±1.5 fold and statistically significant genes are observed above the horizontal line, which corresponds to a *p*-value of 0.05 (Student's *t*-test, $n = 5$ mice per group). A complete list of genes and *p* values are provided in the Supporting material (Supplementary Table 2).

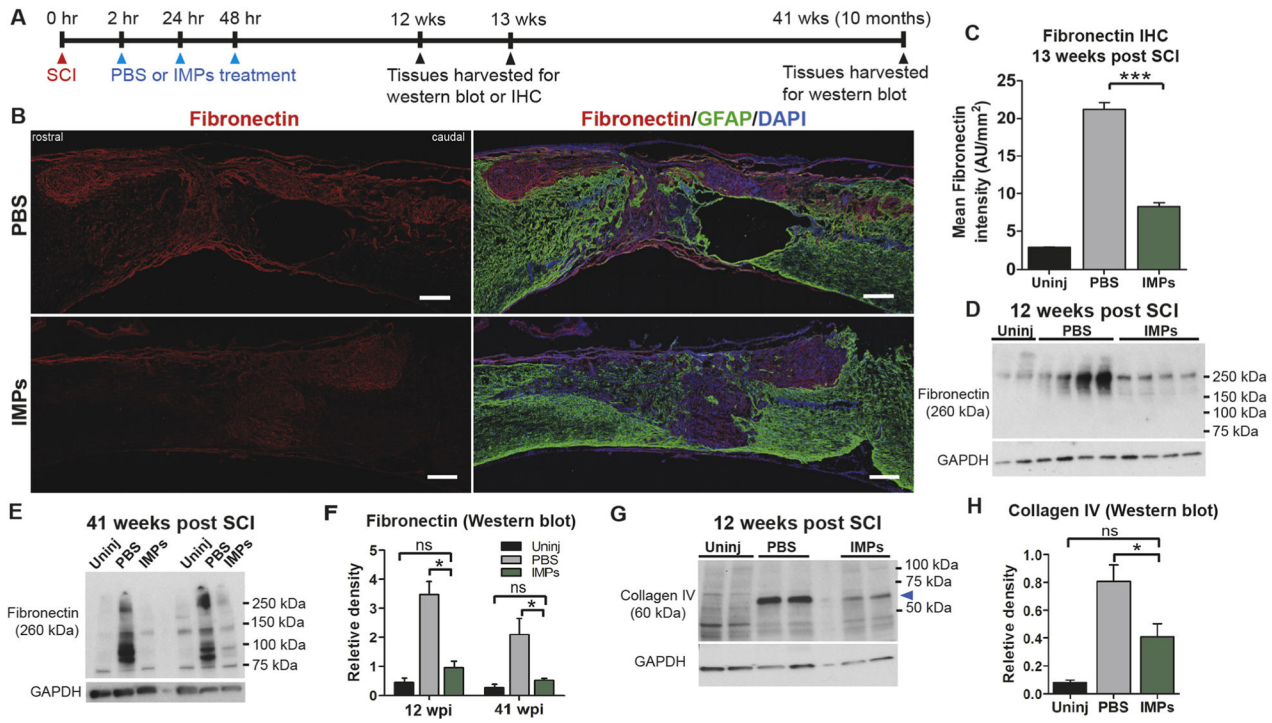

Fig. 3.

IMPs treatment attenuates chronic fibrotic scarring. (A) Experimental timeline. (B) At 13 weeks post SCI, 16 μm thick mid-sagittal sections, identified by the central canals, were obtained from PBS treated or IMPs treated mice and stained with fibronectin and GFAP. Scale bar = 250 μm. (C) Quantification of fibronectin staining inside the lesion. Lesions were identified as $GFAP^-$ areas ($n = 4–5$ mice per group, $^{***}p < 0.001$, ANOVA with Bonferroni's multiple comparison test). (D, E) Western blot analysis of the 1 mm lesion-containing segments of uninjured (Uninj), PBS treated, and IMPs treated mice harvested (D) 12 weeks and (E) 41 weeks post SCI ($n = 4$ mice per group). (F) Western blot quantifications for fibronectin at 12 weeks and 41 weeks post SCI. (G, H) Western blot analysis of the spinal lesions from uninjured (Uninj), PBS treated, and IMPs treated mice at 12 weeks post SCI show significantly reduced levels of collagen type IV ($^*p < 0.05$, ANOVA followed by Tukey's multiple comparison test).

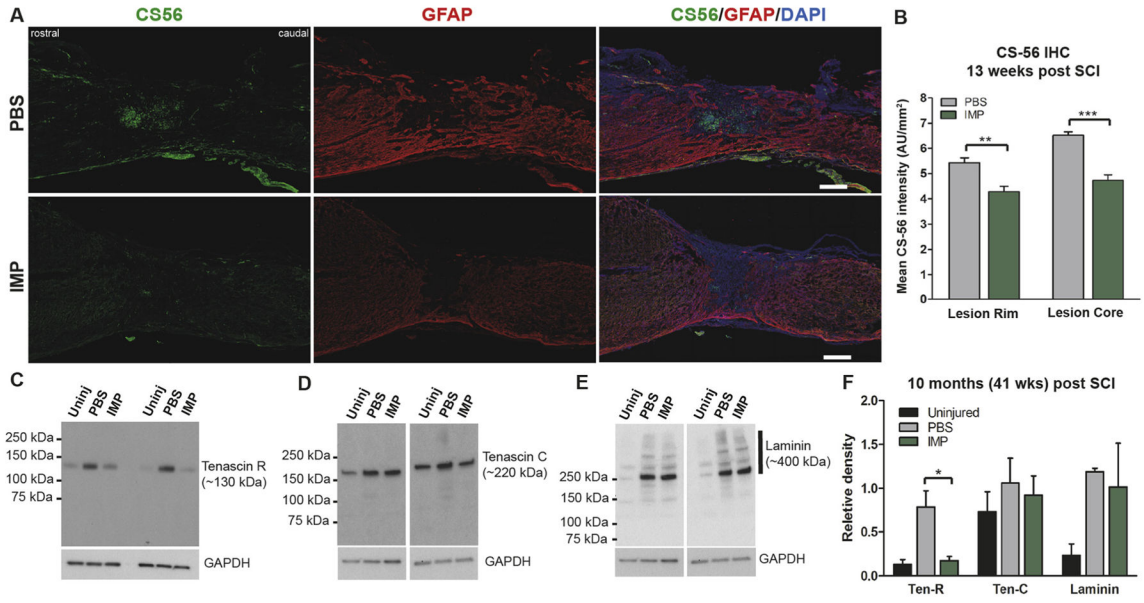

Fig. 4.

IMPs treatment reduces chondroitin sulfate proteoglycan (CSPG) accumulation. (A) Representative images of 16 μm thick mid-sagittal sections of PBS or IMPs treated animals 13 weeks post SCI stained with CS-56 and GFAP. Scale bar = 250 μm (B) Quantifications of CS-56 intensities in the $GFAP^-$ lesion core (Lesion Core) and in the 250 μm wide $GFAP^+$ glial border area that immediately surrounds the lesion (Lesion Rim) ($n = 3$ mice per group, $^{**}p < 0.01$, $^{***}p < 0.001$, Student's t-test). (C) Western blot analysis of the protein samples obtained from the 1 mm lesion-containing segments of spinal cords treated with PBS or IMPs at 41 weeks post SCI ($n = 3$–5 per group) show reduced levels of tenascin R after IMPs treatment. (D, E) IMPs treatment did not alter levels of either tenascin C or laminin 41 weeks post SCI ($n = 3$–5 per group) (F) Quantification shows that IMPs treatment reduced levels of tenascin R but not tenascin C or laminin 41 weeks post SCI ($n = 3$ mice per group).

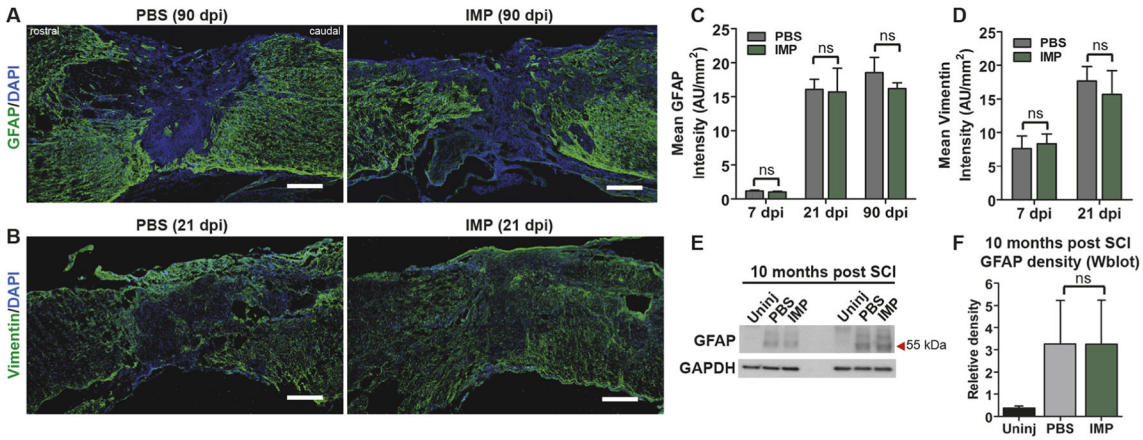

Fig. 5.

IMPs treatment does not affect astrocyte activation or glial scarring. (A, B) 16 μm thick mid-sagittal sections were taken at various time points after SCI and stained with GFAP and vimentin. Quantification of GFAP (C) and vimentin (D) staining inside the lesion core demonstrates no difference in signal intensity between PBS and IMPs treated animals at a range of time points from 7 to 90 days post-SCI. (n = 3–4 per group, Student's t-test). (E, F) Immunoblots of protein harvested 41 weeks post SCI show unchanged GFAP levels between treatment groups. (n = 3 per group, ANOVA followed by Tukey's multiple comparison test). All data are mean ± SEM.

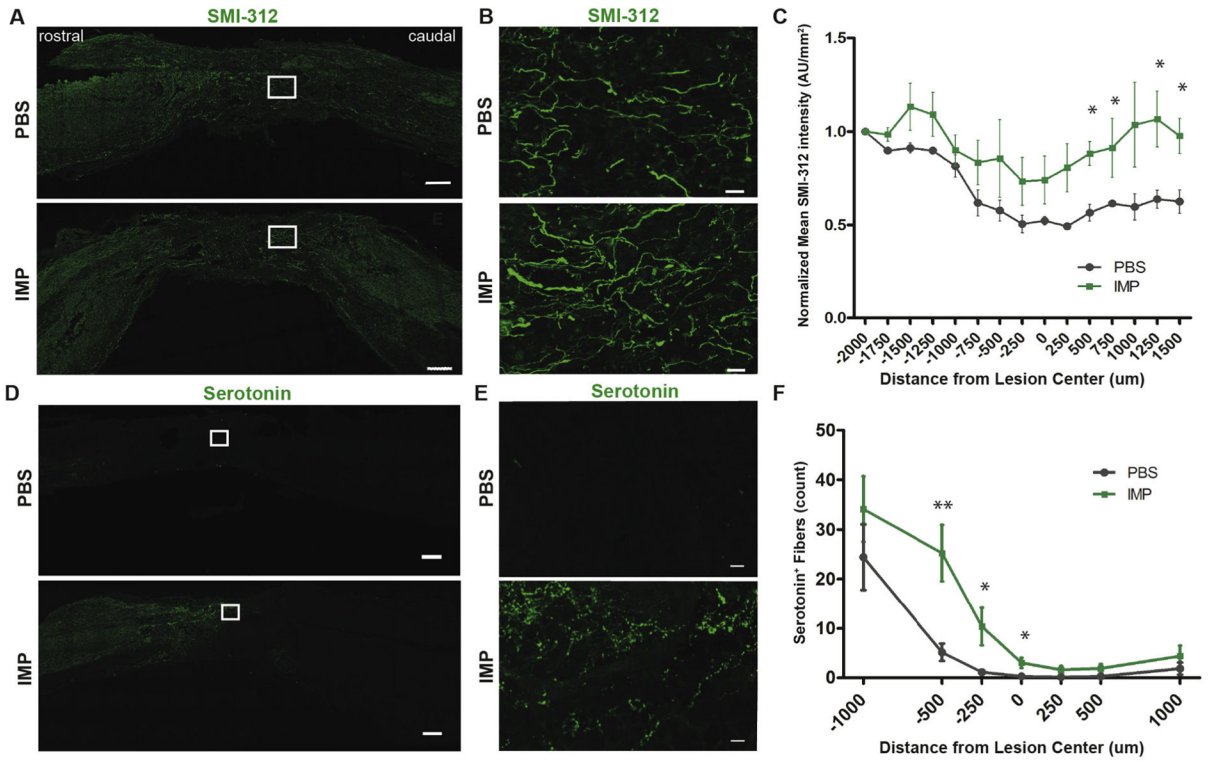

Fig. 6.

IMPs treated animals have higher axonal density both within and caudal to the lesion site. (A) Representative images of 30 μm thick mid-sagittal sections of PBS or IMPs treated animals 26 weeks post SCI stained with SMI-312. Scale bar = 250 μm (B) Enlarged images from the outlined lesion areas. Scale bar = 20 μm. (C) SMI-312 staining intensity is increased caudal to the lesion site in IMP-treated mice. ($n = 4$ mice for PBS and $n = 3$ mice for IMPs group. $^{*}p < 0.05$ by unpaired Student's t-test) (D) Representative images of 16 μm thick mid-sagittal sections of PBS or IMPs-treated animals 13 weeks post SCI stained for serotonin (5-HT). Scale bar = 250 μm (E) Enlarged images from the outlined lesion areas. Scale bar = 10 μm. (F) 5-HT^{+} fibers are more numerous within and immediately rostral to the lesion core in IMP-treated animals as compared to control. ($n = 8$ mice per group) All data are presented as mean ± SEM. $^{*}p < 0.05$, $^{**}p < 0.01$ groups compared by Student's t-test. Distances rostral to the lesion center are defined as negative numbers, while distances caudal to the lesion center are defined as positive.

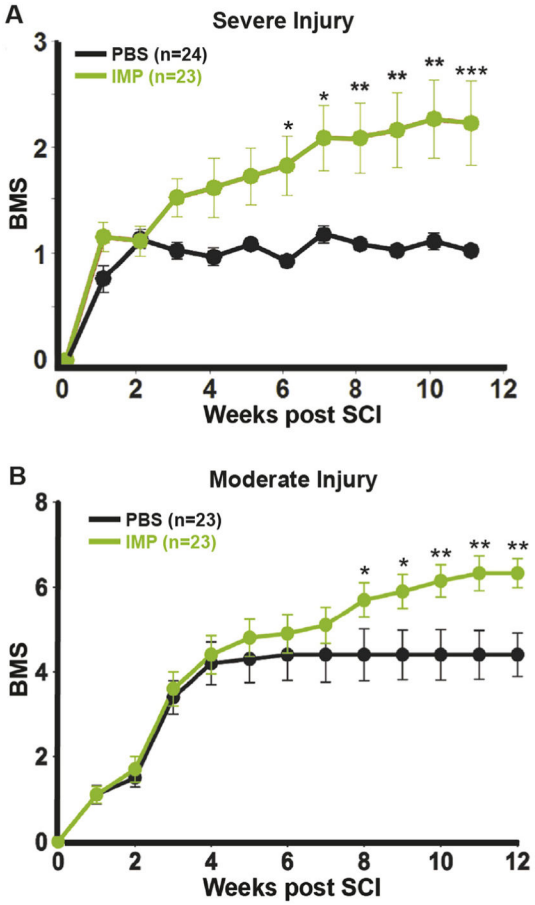

Fig. 7.

IMPs treatment significantly improves motor recovery after SCI. Mice were treated with PBS or IMPs at 2, 24, and 48 h post SCI, and locomotor function was evaluated once every week using the Basso Mouse Scale (BMS). (A) BMS scores following a severe spinal contusion injury, 100 kdyn and 60 s dwell time. (B) BMS scores following a moderate spinal contusion injury, 60 kdyn with 0 s dwell time. All data are presented as mean ± SEM. *$p < 0.05$, **$p < 0.01$, ***$p < 0.001$ with groups compared by two-way repeated measures ANOVA.